J. of Fire Prot. Engr., 5 (4), 1993, pp 147–162

DETECTION OF OCCLUSION AND WALL DEGRADATION IN FIRE PROTECTION PIPING SYSTEMS USING NON-INVASIVE GAMMA-RAY TECHNIQUES

Mansour Alipour-fard, P.E.
University of Colorado, Boulder, CO

John A. Mayer, Jr., P.E.
Worcester Polytechnic Institute, Worcester, MA

Richard L.P. Custer
Worcester Polytechnic Institute and Custer Powell Inc., Wrentham, MA

SUMMARY

Water piping occlusion categories are reviewed. Determination of sprinkler piping occlusions and pipe wall degradation are investigated by using a non-invasive gamma-ray scanning technique. Theoretical and experimental investigations illustrate that the technique is capable of revealing the thickness, location, density and shape of substantial solid occlusions without requiring any prior knowledge about the pipe interior. Major degradation of the pipe wall can also be determined with this technique, provided the scanning speed and collimator thickness are selected properly. While theoretically feasible, determination of thin and porous occlusions could not be achieved experimentally. In theory, if the beam of gamma-ray is very thin and the scanning speed is very small, thin and porous occlusions can be detected.

INTRODUCTION

Acceptable performance of automatic sprinkler systems requires that the piping be able to deliver water at or above the design flow rate and pressure. Over time the interior surface of the piping becomes more rough and the hydraulic diameter may be reduced due to different types of occlusion.[1] Such occlusions reduce water flow and consequently increase the size of fire damage in sprinklered fires.

A detailed analysis of 3,134 cases of unsatisfactory sprinkler performance revealed 200 instances, approximately 7.0 percent, of either plugged heads or obstructed piping.[2] Another source reported that piping obstruction represented 5.6 percent of the causes of unsatisfactory sprinkler performance from 1970 to 1974.[3] A non-invasive technique is required to determine the interior condition of piping. Such a technique will help analyze the availability of water for satisfactory performance of sprinkler systems.

To date, there is no non-invasive technique to assess the amount, location, and shape of occlusion in automatic sprinkler piping. The authors of this paper recognize that many physical principles may be employed to detect piping occlusion. The principles include heat transfer/infra-red radiation, fluid mechanics, ultrasonic physics, and gamma-ray absorption and scattering. In fact, commercial products are currently available which use ultrasonic principles to determine the remaining wall thickness of corroded pipes.

The authors decided to study the feasibility of one physical principle. Previous background of professors Mayer and Custer directed this research effort towards gamma-ray techniques. Professors Mayer and Custer proposed to the National Science Foundation (NSF) that the feasibility of the use of a non-invasive gamma-ray technique in the assessment of sprinkler piping occlusion be investigated. NSF approved the

proposal and funded the project under grant number MSS-861 3561. The approval of the proposal by NSF was followed by a Master of Science Thesis work at the Center for Firesafety Studies of Worcester Polytechnic Institute (WPI). Additional funding was provided by the National Fire Sprinkler Association (NFSA). The research work started in September 1986 and ended in February 1988.[4] This paper presents a summary of that work including a brief overview of water piping occlusion and the gamma-ray techniques explored.

Occlusion In Automatic Sprinkler Piping

Occlusion, blockage, postprecipitation, and obstruction have been used interchangeably in literature to define the existence of physical barriers to water flow in piping systems. For consistency, the term "occlusion" is used in this paper to indicate partial or total obstruction of water flow.

Possible piping occlusion geometries are classified in Figure 1 to provide a uniform nomenclature in this report. As shown, occlusion may be full or partial. Partial occlusion may be circumferential, asymmetric, segmental, or irregular. Full and partial occlusions can be continuous or localized.

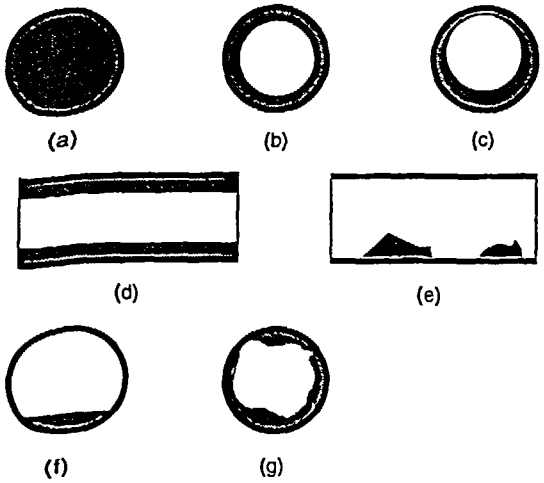

Figure 1. Occlusion Geometry Nomenclature: (a) Full Occlusion, (b) Circumferential, (c) Asymmetric, (d) Continuous, (e) Localized, (f) Segmental, (g) Irregular.

Water piping occlusion are traced back to two general sources: foreign solid objects and particles entering the piping; and solid material forming within the piping, see Figure 2.[1] Foreign material entering the piping include lump objects and material carried in suspension by water which settles in stagnant or low velocity water. Solid material forming within piping system are: water frozen in piping, soft layers of slime on pipe surfaces, corrosion products ranging from small blisters to large tubercles, and postprecipitation of previously soluble chemicals. Postprecipitation products may remain in their place of generation or break and settle elsewhere in the system.

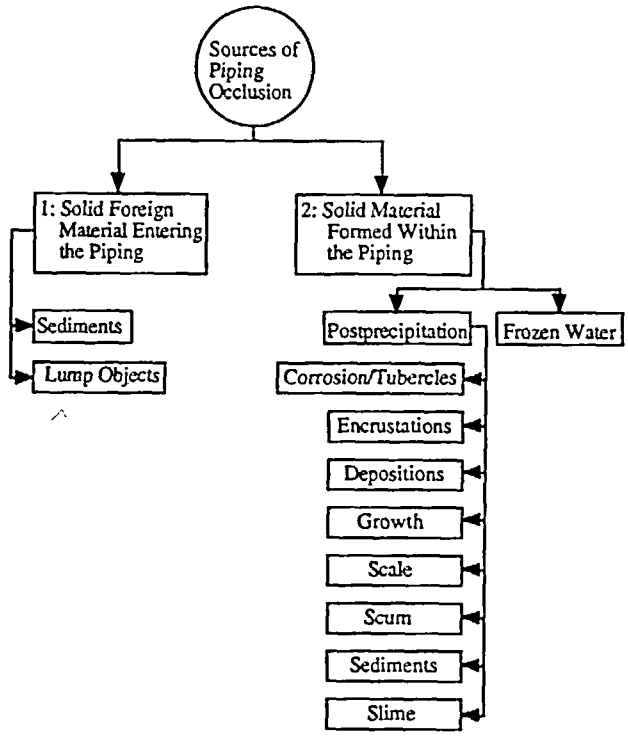

Figure 2. The two major sources of piping occlusion and their categories.

Issues of interest for each category of occlusion include geometry, cause and formation process, effects of pipe material, effects of water impurities, and degree of structural damage imposed on piping. An overview of these occlusion categories is presented on the next page.

Occlusion Categories

Precipitation and Postprecipitation

Precipitation is a process used in water treatment. It involves the reaction of a soluble chemical with chemical compounds naturally present in water to form an insoluble chemical compound. Solid particles thus formed can be extracted from the water.[5]

Precipitation is an intentional phase of the treatment process. However, not all soluble chemicals are extracted from water as it leaves the treatment plant. Unintentional precipitation occurs when chemicals existing in a water react with the new environment in the distribution piping.[5] Consequently, precipitation of certain compounds can occur after water has been treated, thus the term postprecipitation.

The term postprecipitation is sometimes used to describe piping occlusion including sedimentation and corrosion. Iron postprecipitation, for example, is sometimes used to refer to corrosion of iron piping.

Major types of postprecipitation comprise calcium carbonate, iron, lead, zinc, aluminum, magnesium, polyelectrolytes, manganese, and microbiological.[5] Postprecipitation is normally irregular and continuous along the length of the piping. Depending on its type, postprecipitation can cause different levels of damage to the piping. Table 1 illustrates some of the attributes of different types of postprecipitation.

Calcium Carbonate Postprecipitation

Deposition of calcium carbonate ($CaCO_3$) is often used to form a corrosion resistant coating on the pipe interior. However, excess deposition of $CaCO_3$ adversely impacts water carrying capacity of water piping.[5] After the initial protective coating of $CaCO_3$ is formed, efforts should be made to prevent further introduction of the material. Postprecipitation of $CaCO_3$ is normally irregular in shape and can cause continuous occlusion along a length of piping, but is unlikely to cause structural damage.

Relatively accurate predictions of postprecipitation rates can be made using the Langelier Index, also known as $CaCO_3$ Saturation Index.[5]

TABLE 1 Some Attributes of Different Types of Postprecipitation

TYPE OF POST-PRECIPITATION	AFFECTED BY WATER IMPURITIES	AFFECTED BY PIPE MATERIAL	CAN CAUSE OCCLUSION IN PIPING	CAN CAUSE SERIOUS DAMAGE TO PIPING
Calcium Carbonate	Yes	NS	Yes	NS
Iron	Yes	Yes	Yes	Yes
Zinc and Lead	Yes	NS	Yes	NS
Aluminum	Yes	NS	Yes	NS
Magnesium	Yes	NS	Yes	NS
Polyelectrolyte	Yes	NS	Yes	NS
Manganese	Yes	NS	Yes	NS
Microbiological	Yes	Yes	Yes	Yes

NS= Not Studied

When predicting postprecipitation of $CaCO_3$ factors such as calcium concentration, alkalinity, dissolved solids, and water temperatures must be taken into account.[5]

Corrosion

Most sprinkler piping occluded by the process of corrosion is ferrous. While corrosion may attack the interior and/or exterior of piping, we have limited this overview to interior corrosion of ferrous pipes.

The geometry of corrosion is normally irregular and, depending on the type of corrosion, may be continuous or localized. The formation process is chemical and/or biological. Pipe material and water temperature, acidity, and impurities affect type and rate of corrosion. Corrosion, in particular pitting corrosion, can cause structural damage to the pipe.[6]

The initial corrosion reaction is an electrochemical one and may be explained as the displacement of a metal ion from an anodic site on the metal surface to a site in the solution which leaves behind a number of excess electrons; concurrently, electrons are consumed at a nearby cathodic site.[7] Oxygen availability, *e.g.*, through the introduction of fresh water, enhances the rate of corrosion.

The corrosion process can reduce the thickness of the pipe wall and generate tubercles, scales, and loose particles. Holler[6] and Rothwell[7] explain several types of corrosion in water piping including uniform, grooving, pitting, tuberculation, exfoliation, water-line attack, crevice attack, dezincification, corrosion erosion, galvanic corrosion, and graphitization. Tuberculation can cause major occlusion of iron piping and is explained below. Review of other forms of corrosion is beyond the scope of this work. Briefly, water-line attack is a type of corrosion that takes place at the point where air, water, and metal intersect. A typical example is a drop of water on an iron surface, *e.g.*, interior of a dry pipe sprinkler system following a trip test.

Tuberculation

In 1950, Olson and Sybalski found that the tubercle formation initiated by bacterial growth on pipe walls was the critical factor on the internal corrosion of iron pipes.[8] Iron bacteria such as *Gallionella* may add to the problem of tuberculation without being involved in the corrosion process by metabolizing ferrous ions already present in the solution and laying down large masses of ferric oxide on the sheath of the organism.[7,8]

Tuberculation of iron pipes is an electrochemical/biological process affected by water quality. This type of piping occlusion is normally expected to be continuous along a length of pipe and irregular in shape. Corrosion products forming on the inner surface of piping often resemble tubercles, thus the term tuberculation. The mechanism involves oxidation of ferrous hydroxide to hydrated ferric oxide. The ferric oxide forms layers and blisters often interlaid with calcium, iron and other metallic salts. Often a hard surface coating of Fe_3O_3 forms, providing the main structure of grown tubercle.[6-8]

Sedimentation

In the context of open channel hydraulics, sediment is defined as material carried in suspension by water which would settle at the bottom of the channel if water lost velocity.[9] While substantial research has been conducted on different aspects of open channel sedimentation, authors of this paper were unable to find published correlations for the rate of sedimentation and settling velocity in the context of water piping.

The geometry of pure sedimentation is expected to be segmental. However, when combined with other categories of occlusion, the geometry may become irregular, but thicker and more dense at the bottom of the pipe. Sedimentation is either continuous along a length of the pipe or localized, *e.g.*, when pipe changes direction. Sedimentation causes occlusion to water flow, but will not directly cause structural damage to piping.

While the initial process forming the sediment deposits is diverse, the settling process is a physical one. As indicated in Figure 2, sediment in automatic sprinkler piping comes from two major sources. The first source is the suspended materials carried by water from outside the system. Poor water treatment and penetration of soil into the piping, *e.g.*, during repair, are typical causes for the presence of suspended material. The second source is the postprecipitation products generated within the piping which may remain in their place of generation or break and settle elsewhere in the system, *e.g.* due to decrease in water velocity or change in the direction of water flow from horizontal to upward vertical. *The Fire Protection Handbook* [10] reports that sprinkler piping occlusions usually consist of concentrations of the lighter material such as silt and sand in the ends of the cross mains and in the nearby branch lines and heavier solids near the system risers.

Lump Objects

Lumps and unusual objects such as plumbing hardware, pieces of wood, and "pipe coupons", cut and dropped into piping during system installation, are typically caused by human error. Their geometry is expected to be irregular and localized. While capable of causing serious localized occlusion, lump objects alone are unlikely to cause structural damage to the pipe.

Objectives Of This Study

Recommended practice for maintenance of sprinkler systems[3] calls for flushing of the system and water flow tests on a periodic basis. While these can loosen and flush out some scale and sediment, flushing and water flow tests will also bring in fresh water which will enhance corrosion. Also, depending on its quality, fresh water can introduce additional dissolved mineral matter and/or suspended particles that could further increase sedimentation and postprecipitation.

While it is often possible to clean the piping, the present means for determining whether to clean or possibly replace the system is a complicated and costly process which involves partial disassembly of the system for visual inspection. Moreover, this method lacks the capability for measuring the existing hydraulic diameter of the pipe, finding localized occlusions, finding localized pitting of the pipe wall, and determining the shape of occlusion. Determination of the shape of occlusion, for example, could give a clue to its nature, *e.g.*, sedimentation versus tuberculation, and hence dictate the method of cleaning. In addition, finding localized occlusions and localized pitting of the pipe wall could suggest that only partial replacement of the system is necessary.

This study investigated the feasibility of the use of gamma-ray techniques to determine the presence, shape, and size of piping occlusion and possibly the remaining thickness of the pipe wall. In addition, the team noted that potential health hazards of the technique, to operators and the general public, should be investigated. Following the establishment of the objectives, theoretical and experimental efforts were directed towards securing the objectives.

Theoretical Studies

The theoretical feasibility studies consisted of two stages: geometrical analysis (pipe and occlusion geometry); and gamma-ray techniques.

In practice, the process involved trial and error between the two stages. For example, after initial completion of geometry stage and during the gamma-ray analysis, the team noted that there are unknowns that can be further simplified by specific geometrical analyses. This report presents the final outcome and does not cover the trial-and-error process between the two stages.

Geometrical Analysis

To simplify the analysis, this stage was aimed at studying the dimensional relationships in a circumferentially occluded pipe. Effectively, this would be a concentric three-layer cylinder with pipe wall, occlusion, and water forming the three layers. As illustrated below, the thickness of a barrier through which a beam of monoenergetic gamma-ray passes directly affects the attenuation of that beam. Therefore, this section is to provide correlations for the calculation of the effective thickness of each layer of the subject cylinder at different points.

Using basic geometric relations for cylinders, it can be shown that Equations 1 through 3 apply to the three-layer cylinder of Figure 3. In these equations, t is the effective thickness of each layer and is a function of elevation, h, see Figure 3. Elevation, h, as shown in Figure 3 is the vertical distance from the surface on which the pipe is laying to the location of interest.

One may visualize that the three-layer cylinder of Figure 3 is being cut along its length with a flat horizontal cutting surface at elevation h. The effective thickness of each of the three media (t_1, t_2, t_3) is defined as the total thickness of that media which is in contact with the visualized cutting surface at the given elevation. Note that in Equations 1–3, t_1, t_2, t_3, h, R_1, R_2, and R_3 all have the units of length (cm). Note: t_2 and t_3 change with elevation, h.

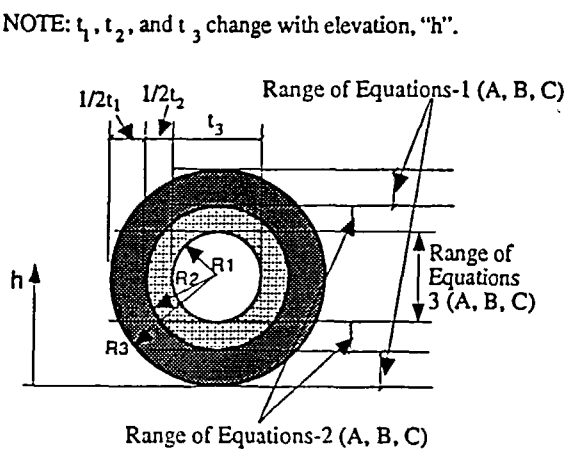

Figure 3. Dimensional correlations in a three-layer cylinder (range of Equations 1, 2, and 3).

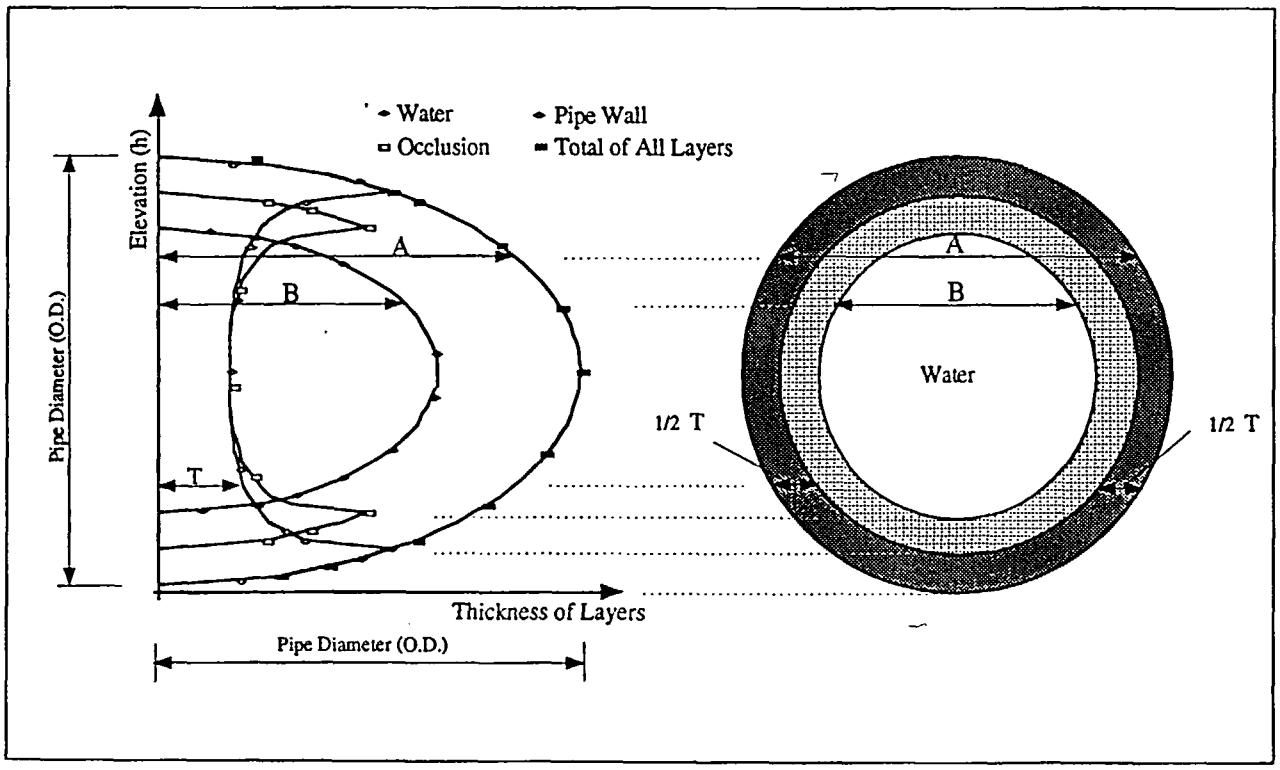

Figure 4. Plot of effective thickness vs. elevation for different layers of a three-layer cylinder.

For 0 h (R_1-R_2) and (R_1+R_2) h 2R_2:

$$t_1=(8R_1h-4h^2)^{1/2} \quad (1A)$$

$$t_2=0 \quad (1B)$$

$$t_3=0 \quad (1C)$$

For (R_1-R_2)<h (R_1-R_3) and (R_1+R_3) h<(R_1+R_2):

$$t_1=(8R_1h-4h^2)^{1/2}-t_2 \quad (2A)$$

$$t_2=(8R_2(h-R_1+R_2)-4(h-R_1+R_2)^2)^{1/2} \quad (2B)$$

$$t_3=0 \quad (2C)$$

For (R_1-R_3)<h< (R_1+R_3):

$$t_1=(8R_1h-4h^2)^{1/2}-t_2-t_3 \quad (3A)$$

$$t_2=(8R_2(h-R_1+R_2)-4(h-R_1+R_2)^2)^{1/2} \quad (3B)$$

$$t_3=(8R_3(h-R_1+R_3)-4(h-R_1+R_3)^2)^{1/2} \quad (3C)$$

Using the above equations, a plot of the effective thickness, t, vs. elevation, h, for each layer of a three-layer cylinder and the total thickness of all three layers are displayed in Figure 4. Similar correlations and graphs can be developed for other related geometrical shapes such as asymmetric and segmental type occlusions.

Gamma-Ray Absorption and Scattering

As a mono-energetic beam of gamma-ray passes through an absorber, *i.e.* a barrier, its intensity drops as a decaying exponential function of the absorber thickness and an absorber material property known as the *linear absorption coefficient*, μ_1. The absorption/scattering of gamma-rays is via three mechanisms: pair production, Compton effect, and photoelectric effect. Review of these mechanisms is beyond the scope of this work. The complete effect can be summarized in the following equation.[11]

$$I = I_0 e^{-\mu_1 t} \quad (4)$$

Where: I_0= Initial Flux Intensity of the Beam (Photons/sec.)
I = Flux Intensity of Beam after Absorption, *i.e.* Uncollided Photons (Photons/sec.)
μ_1= Linear Attenuation Coefficient of the Absorber (cm^{-1})
t = Thickness of Absorber (cm)

For an absorber made of several different material, *e.g.*, a three layer cylinder, see Figure 5, Equation 5 should replace Equation 4. Subscripts 1, 2, and 3 refer to the three media/layer.

$$I = I_0 e^{-(\mu_{1.1}t_1+\mu_{1.2}t_2+\mu_{1.3}t_3)} \quad (5)$$

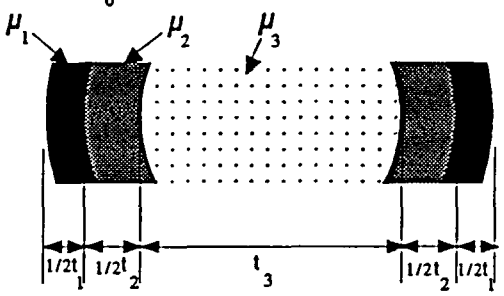

Figure 5. A portion of a three-layer cylinder through w hich a beam of gamma-ray is passing.

In Equation 5 the intensity of incident beam, "I_0", and that of the beam after going through the pipe, "I", can be measured. Also, the linear attenuation coefficient of water and pipe material are known. However, recalling that the technique is to be non-invasive and the pipe is to remain closed, the occlusion thickness (t_2), the linear attenuation coefficient of occlusion ($\mu_{1.2}$), and the remaining thickness of pipe wall (t_1) are unknown. Therefore, containing three unknowns, Equation 5 alone cannot provide us with the occlusion thickness. Note that the thickness of water layer was not listed among unknowns since the exterior diameter of the pipe is known. Once the thickness of two layers (t_1 and t_2) and the external diameter of the pipe (t_1+t_2+t_3) are known, t_3 can be obtained by substraction.

If Equation 5 could be solved, the theoretical studies would have reached a resolution. As explained in the previous paragraph, this resolution was not to be. How-

ever, at this stage, a question was raised as to whether there is a need to solve this equation. Instead, the team decided to look into the use of Equation 5 to construct a topographical map showing the combined impact of the effective thickness and the attenuation coefficient across the pipe.

The factors affecting the linear attenuation coefficient are the mass density (referred to as "density" throughout this paper), and the atomic number of the absorbing media. However, it can be shown that, for photon energies of approximately 0.4 to 4.0 Mev, μ_1 is nearly independent of the atomic number of the intervening media and is predominantly dependent on the density (g/cm^3) of the intervening media.[12] Based on this view of the linear attenuation coefficient, the construction of the subject topographic map appeared viable.

Using Equations 1–3, and multiplying the thickness of each layer by the density of that layer, a graph of (Thickness x Density) Vs. (Elevation) was constructed (see Figure 6 and compare with Figure 4). This plot is for a steel pipe, circumferentially occluded with a homogeneous material with a density of 2.0 g/cm^3, and water, 1.0 g/cm^3, inside the pipe. This procedure and the resulting graph, Figure 6, formed the basis of the "Parallel Beam Gamma-Ray Scanning."

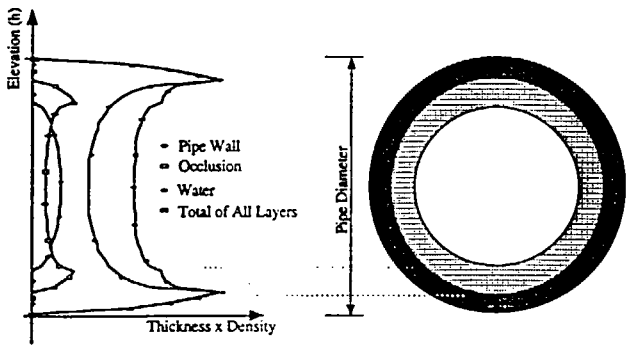

Figure 6. Plot of "Thickness x Density" vs. "Elevation" (h) for a three-layer cylinder.

Parallel Beam Gamma-Ray Scanning

The principles used in the construction of Figure 6 were also used to hypothesize the scanning technique. In this technique, a collimated mono-energetic beam of gamma-ray of a known intensity is passed through the pipe. The uncollided gamma-rays, *i.e.*, photons with the same energy as the incident beam, are counted as they depart from the other side of the pipe. Up to this point, the process is similar to the simple use of Equation 5 but in this case the process is repeated by making a traverse normal to the pipe centerline from bottom of the pipe to the top, *i.e.* parallel scanning across the pipe. Figure 7 illustrates this scanning procedure. The resulting data, from the detector, can be used to construct a plot of the beam position (h) versus departing flux intensity of the gamma-ray beam (I).

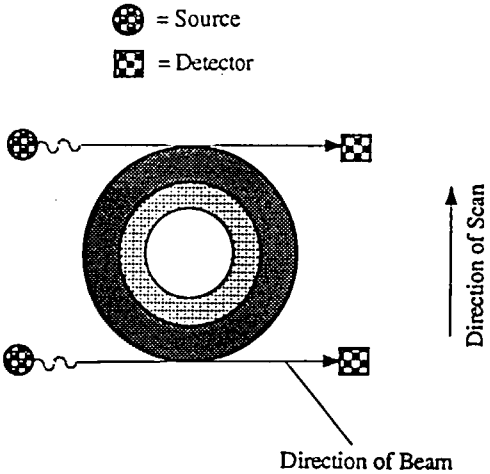

Figure 7. Gamma-ray traces through pipe.

This technique takes advantage of two facts: that the amount of attenuation of a beam of gamma-rays depends on the densities and thicknesses of the intervening media; and that the thicknesses of different layers of a multilayered cylinder change with elevation h.

As noted earlier, the linear attenuation coefficient is largely a function of density in the range of energies proposed. Therefore, based on Equation 5 the intensity of the departing beam (I) has a decreasing

exponential relation with the product of thickness and density of the absorbing media. The decaying function suggests that a plot of I Vs. *h* should resemble the mirror image of Figure 6.

Using Equation 5 as the governing gamma-ray absorption equation and Equations 1–3 as the governing geometric relations, a computer program was written to investigate the theoretical feasibility of the technique.[13] Using that computer program, extensive theoretical feasibility and sensitivity studies were conducted. The studies included computer modeling of occluded and non-occluded pipes of different size, circumferentially occluded with various thickness and density occlusion material. The computer models included air or water inside the pipe. These studies illustrated the theoretical feasibility of the approach. A sample of the computer output plot is given in Figure 8; compare with Figure 6. Visual examination of such plots reveals the occlusion.

The theoretical feasibility studies were limited to circumferentially occluded pipes with homogeneous occlusion material. However, experimental studies covered a wide range of pipe and occlusion geometries.

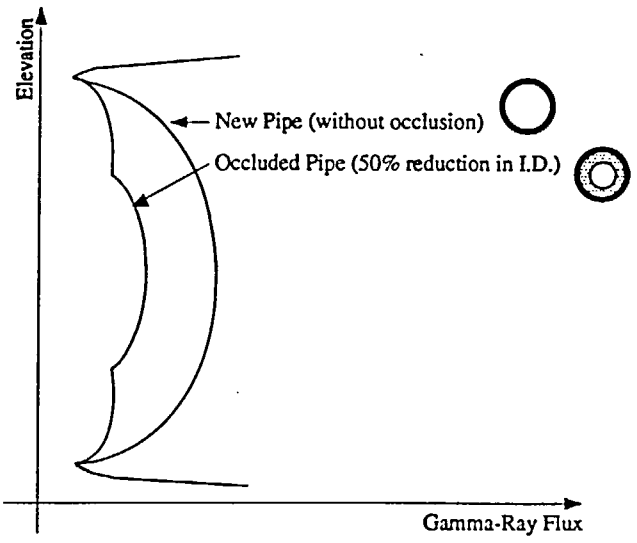

Figure 8. Computer simulations of gamma-ray scanning across a circumferentially occluded pipe and an occlusion-free pipe.

Longitudinal Gamma-ray Scanning

Unlike the case of moving across a cylinder (see "Geometrical Analysis"), the thickness of each layer of a three-layer cylinder remains constant as a point moves along the cylinder axis. Therefore, based on Equation 5, with the thicknesses, attenuation coefficients and incident beam remaining constant, the value of "I" remains constant as the source and detector move along the cylinder. In other words, if a pipe is symmetrically occluded with a material of uniform density, its longitudinal scan plot will be a horizontal line. Any change in the uniformity of thickness of layers or their densities will affect the shape of the plot. For example, if the cylinder or pipe is occluded by a lump object, the longitudinal scan plot will show marked decrease at that point.

Experimental Design

The Test Apparatus and Experimental Procedure

A schematic diagram of the test apparatus is shown in Figure 9. This apparatus was designed for scanning across the pipe. With the setup shown in Figure 9 the detector and the source are stationary, while the pipe (sample) is moving at a constant speed. The difference between this setup and any practical application is that in this setup the pipe moves while the source and detector remain fixed. In field investigations, the pipe is fixed and the source/detector assembly must move. Both methods will result in the same outcome since in both cases the pipe moves relative to the apparatus.

The source emits a collimated beam of gamma-rays towards the detector while the pipe moves across the beam (see Figure 4). The signal received by the detector is then sent to a Multi Channel Scaler (MCS). The MCS is provided with means to filter photon energies above and below a certain range, *i.e.*, by means of upper

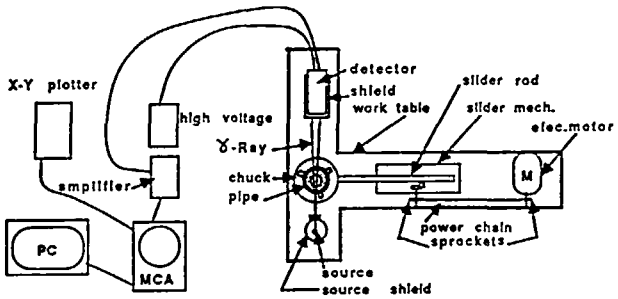

Figure 9. Schematic diagram of the experimental setup.

and lower level discriminators (ULD and LLD). ULD and LLD should be set such that only uncollided gamma-rays will be counted. Using the number of detected gamma-rays at each scan position, the MCS makes a plot of the number of photons vs. the scan position (h). To create a hard copy of the scan, a plotter is attached to the MCS. Several examples of the plotter output are given later in this paper.

A computer program was written so that the MCS could communicate with a personal computer. The number of counts for each channel, representing (I) in Equation 4, along with the channel numbers, representing h in Equations 1–3, are transferred to the PC. The data was restored on disk for later analysis.

The apparatus consisted of the following components:

- A *Pipe Moving Mechanism* which consisted of a chuck, a slider mechanism, and an electric motor. Scanning speeds used in this study ranged from 0.6 to 15.0 cm/min.

- The *Shielded Gamma-ray Source* was a 24.0 mCi-Cs^{137}. A second source, 0.6 mCi-Co^{60}, was also used in some experiments to investigate the effect of source strength.

- A *Source Collimator*, made of lead, was used to direct a thin beam of gamma-ray towards the detector. Geometrically, two types of collimators were used: circular and rectangular/slit shaped.

- The *Detector Window*, in the lead shield around the detector, was used to prevent the collided gamma-rays from getting into the detector. This window is geometrically similar to, but proportionally larger than, the source collimator. Note that with the proper setting of ULD and LLD, and adequate separation of the detector from the pipe, the provision of the detector window is optional.

- The *Data Collection* portion consisted of the following elements:
  - a Harshaw™ CR483 Sodium Iodide scintillation detector,
  - a 2010-NUCLEUS™ and later a 451-ORTEC™ amplifier (The two amplifiers resulted different resolutions; The reason for this was not investigated further),
  - a "The Nucleus™ 500-Nuclear Scaler" high voltage supply,
  - a 1056C-DS Davidson™ multichannel scaler/analyzer (MCS/MCA),
  - an Hp™-7035B plotter, a printer, and a personal computer (PC).

Test Samples

Twenty four straight pieces of pipe were selected for the experiments. Twenty three of the samples were Schedule 40 steel pipes from 2.0 to 6.0 inches (5. to 15. cm) nominal diameter. One sample was an 8.0 inch (20.0 cm) cast iron pipe.

Two main categories of occlusion material were utilized, artificial and natural. Materials used for artificial occlusion were plaster of paris and plastic resin whose densities were 1.25 and 1.84 g/cm^3 respectively. The natural occlusion inside the cast iron pipe had a density of 2.0 g/cm^3.

Overall, eighteen of the samples were artificially occluded, three samples had

natural occlusion and the remaining three had no occlusion. Artificial occlusions were made to simulate homogeneous circumferential, multilayered circumferential, and segmental type occlusions, and lump objects. The thicknesses of the artificial occlusion layers ranged from 0.6 to 7.4 cm.

Plaster of paris or plastic resin was cast inside the pipe and machined to a uniform thickness to simulate homogeneous circumferential tuberculation. One layer of plaster of paris and one layer of plastic resin were cast in a 6.0 inch (15.0 cm) nominal diameter pipe to simulate multilayered circumferential tuberculation. Plaster of paris was cast at the bottom of a sample to simulate sedimentation. In one case, a steel rod was set within the plaster of paris casting to simulates a "lump" object.

Among the three samples with natural occlusion one was a tuberculated 8.0 inch (20.0 cm) nominal diameter cast iron pipe where the tuberculation thickness and surface roughness were not uniform. This sample was taken from a 90-year old water main in Worcester, Massachusetts. Two other natural samples were taken from a 2-1/2 inch (6.3 cm) diameter sprinkler system piping. The system's age was undetermined; the pipe's interior was covered with layers of porous corrosion blisters which reduced the hydraulic diameter of piping by 1/2 inch (1.3 cm). The interior surface of one of these samples was machined to achieve a corrosion thickness of 1/16 in (0.16 cm).

Three samples were provided with no occlusion to investigate the feasibility of the technique in assessing wall degradation. The wall thicknesses of two 6.0 inch (15.0 cm) steel pipes were machined to 40 percent and 60 percent of their original value. The third occlusion-free sample was a 2-1/2 inch (6.3 cm) diameter steel pipe with its original wall thickness. This sample was used to investigate the feasibility of this technique in determining the wall thickness of smaller diameter pipes.

Experimental Results

Discussion

The relationship between a sample and its experimental scan plot is shown in Figure 10. The pipe wall thickness, the occlusion thickness, the existing hydraulic diameter are shown in the same scale as the cross section of the sample. The interface between the pipe wall and occlusion (points A and D) and between occlusion and fluid inside the pipe (points B and C) can also be seen.

(a) Pipe Cross Section

(b) Scan Plot

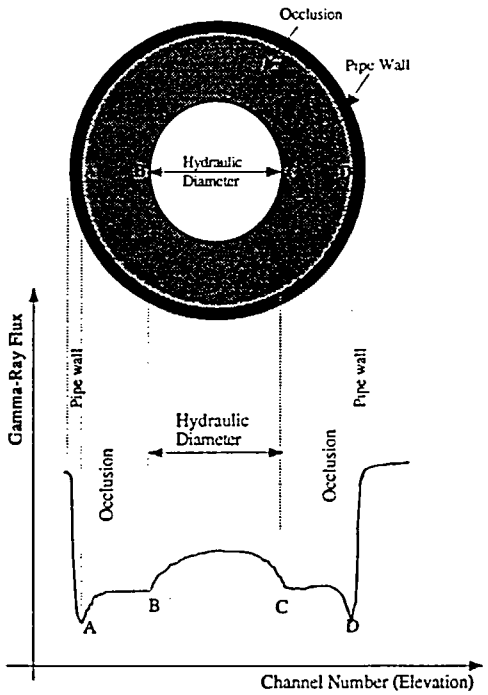

Figure 10. Sample scanning plot.

Resolution of the Scan Plots

Two aspects of resolution that are of interest are the overall smoothness of the plots, and the clarity of the location of the interface between different media/layer in each plot. The term "resolution" is used in this paper to indicate both of these aspects.

The smoothness of the plot was found to be a function of the scanning speed. It can be seen in Figure 11 that a slower scanning speed, *i.e.*, producing more counts per channel, results in a smoother curve and a more well defined indication of the interfaces of interest.

The major purpose of this work, however, was to determine the occlusion thickness, existing hydraulic diameter, and pipe wall thickness. As such, the clarity of the interface between different media on the scan plot becomes a major concern. Although the overall smoothness of the scan plot is a helpful factor in clarity of the interface location, experiments illustrated that smoothness alone may not be adequate (see Figures 11a and 13b). In Figure 11a the plot is not smooth but the occlusion/fluid interface is relatively clear. The interface is less distinct in Figure 13b, although it is a smoother plot.

Experimental Variables

Sensitivity tests were conducted to investigate the effects of the experimental variables on the determination of pipe wall and occlusion thicknesses. The variables included, gamma-ray source strength, collimator geometry, scanning speed, occlusion thickness, occlusion density, fluid inside the pipe, occlusion roughness, and pipe wall thickness.

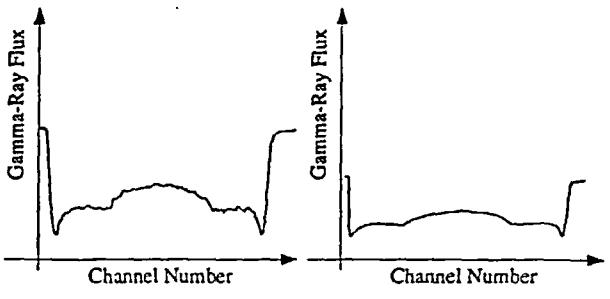

(a) 15.0 cm/sec. (b) 1.0 cm/sec.

Figure 11. Effects of scanning speed on resolution.

Scanning Speed

Lowering the scanning speed increases the number of counts per channel which will in turn decrease the indeterminate errors, and thus produce smoother plots as shown in Figure 11.

Gamma-ray Source Strength

It was found that higher source strength yields a sharper image of the occlusion on the scanning plot, as shown in Figure 12.

As discussed above,smoother plots are also achieved by employing slower scan speeds which produce higher number of counts per channel. As the number of photons increases, *i.e.*, either by increasing the source strength or by decreasing the scanning speed, the indeterminate/statistical errors decrease, resulting a better resolution. The maximum allowable source strength should be dictated by radiological safety considerations which will in turn limit the scanning speed.

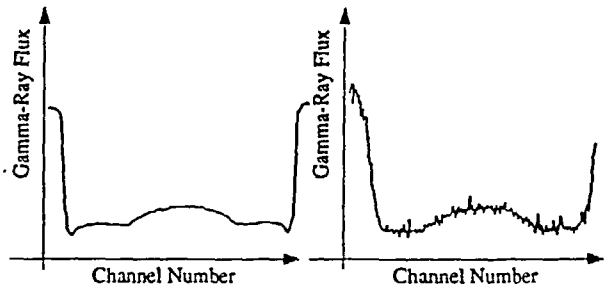

(a) 24.0 mCi Cs137 Source (b) 0.6 mCi Co60 Source

Figure 12. Effects of source strength on resolution.

Collimator Geometry

Two geometrical features of the source collimator proved to be important, area and width. Experiments illustrated that the resolution quality has a direct relationship with area of collimator and an inverse relationship with the collimator width. Enlarging the collimator area causes

an increase in the number of emitted photons and produces a smooth plot. Reducing the collimator width produces more distinct interface locations. Both aspects of resolution improved when the beam was made thinner while maintaining the same or a larger collimator area (see Figure 13).

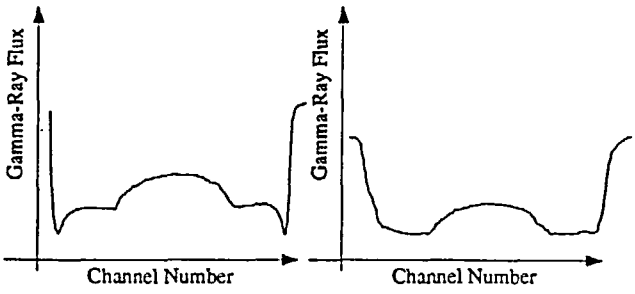

(a) Slit Collimator (0.08x0.71 cm).

(b) Circular Collimator (0.2 cm dia.).

Figure 13. Effects of collimator geometry on resolution.

Occlusion Thickness

The experiments were successful in revealing non-porous occlusions with wall thicknesses as low as 0.6 cm. Smaller thicknesses of artificial occlusions were not investigated. An attempt was made to detect the presence of porous corrosion "blisters," but the resolution achieved was inadequate (even when using the higher source strength combined with slit collimator, and a scanning speed of 1.0 cm/minute). Moreover, although theoretically feasible, experiments could not reveal the thickness of 0.16 cm thick occlusions. More studies are required to determine whether thinner collimators can help detect of thin occlusions.

Occlusion Density

The experiments were successful in revealing occlusions with densities of 1.25 g/cm^3 (for plaster of paris), 1.84 g/cm^3 (for plastic resin), 2.0 g/cm^3 (for natural tubercle), and 7.85 g/cm^3 (for steel rod).

Natural and Artificial Occlusions

Qualitatively, artificial occlusions with a uniform density and a smooth surface resulted a sharp and clear interface while relatively non-uniform natural occlusions with a rough surface produced less distinct interface locations on the scan plot (see Figure 14). These plots are not smooth, possibly due to the nonhomogeneous nature and rough surface of the natural occlusion in this sample. More studies, possibly with thinner slit collimators, are required to investigate the feasibility of using this technique in determining the occlusion roughness.

All of the scanning experiments on artificially occluded samples were in good agreement with the theory set forth in *Theoretical Studies*. Moreover, visual examination of the scan plot revealed the existence and location of occlusion. Figure 10, for example, shows the cross section of a 6 inch (15.cm) diameter empty steel pipe, circumferentially occluded to a hydraulic diameter of 3 inch (7.5 cm) with plaster of paris. The pipe wall thickness, occlusion thickness and available hydraulic diameter is revealed in the scan plot.

Irregularity of the shape and sudden change in the density of occlusion were also discernible in the scan plots. Figure 15, for example, shows the cross section and the scan plot of a 6.0 inch (15.0 cm) diameter steel pipe, circumferentially occluded to a hydraulic diameter of 2-1/2 inch (6.3 cm) with plaster of paris. In addition, a steel rod was located within the plaster of paris casting. The scan plot reveals the sudden change of density, from 1.25 g/cm^3 for plaster of paris to 7.85 g/cm^3 for steel.

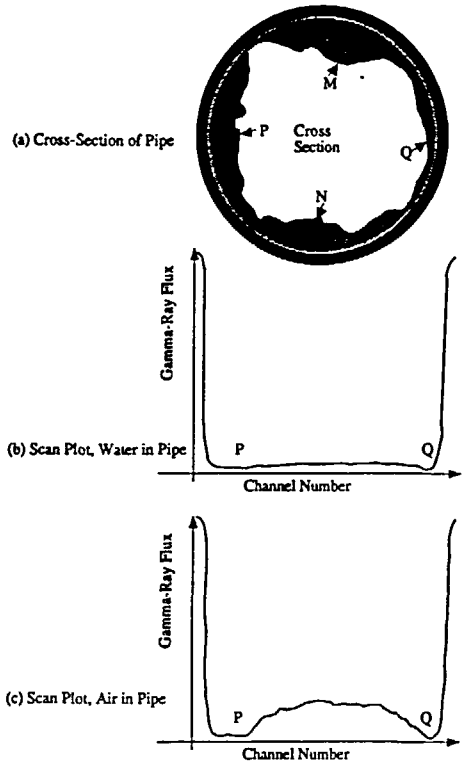

Figure 14. Scanning of a tuberculated (8" I.D.) cast iron sample.

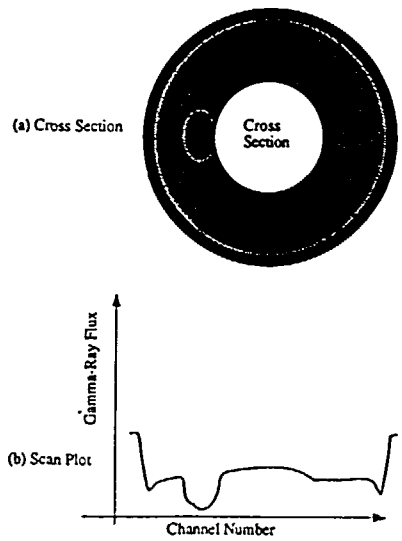

Figure 15. Scanning of lump object occlusions.

Figure 16 shows the cross section and the scanning plot of a sample with segmental occlusion; plaster of paris was used to simulate sedimentation.

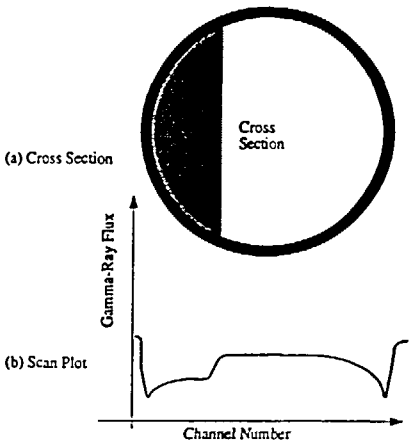

Figure 16. Scanning of segmental occlusions.

A 2-1/2 inch (6.3 cm) diameter sample which was used in an automatic sprinkler system for an undetermined number of years was used in a series of experiments. The interior of the pipe was covered with porous corrosion blisters which reduced the pipe's internal diameter by 1/2 inch (1.3 cm). The scan plot did not give a clear indication of the corrosion blisters. It appears that the cavities within the occlusion blisters have been filled with fluid, making it appear the same to the gamma-ray beam. Note that in theory thin and porous occlusions are detectable. More studies are required to determine whether thinner collimators can help detect of thin/porous occlusions.

Fluid Inside the Pipe

Artificial occlusions were readily detectable with either water or air in the pipe. However, a larger difference between the densities of occlusion and air resulted in a more clear indication of the occlusion interface when there was no water in the pipe. The experiments done with non-porous natural occlusions were also informative (see Figure 14). If the cross section of the pipe was not given, with some visualization one could draw the following conclusions from Figures 14b or 14c:

- The occlusion is thicker at the bottom of the pipe, point P, than the top of the pipe, point Q, possibly due to sedimentation.
- The occlusion has a rough surface and/or is not homogeneous.
- There is no substantial sudden change in the occlusion density.

This experiment could be repeated in another direction to reveal the occlusion thickness at other points, *e.g.*, M and N. Construction of a circle passing through points P, Q, M and N could be used to shed light on the approximate map of the occlusion cross section. If more accuracy is required, scanning of the pipe in additional directions would become necessary.

Pipe Wall Thickness

The pipe wall thickness was detected in all of the experiments where other experimental factors were appropriately selected, *e.g.*, lower scanning speeds and thinner beams for smaller pipes.

Radiological Safety

The horizontal plane of maximum radiation intensity is an imaginary horizontal plane which contains the source. Figure 17 shows the map of maximum radiation intensity, around the apparatus, measured during one of the experiments.

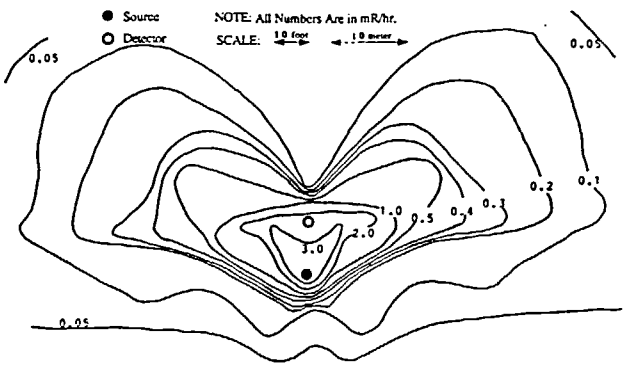

Figure 17. Topographical map of maximum radiation intensity.

Using 5.0 REM/Year and 0.5 REM/Year[12] for occupational and non-occupational allowable radiation doses, one can use Figure 17 to determine the minimum allowable distance to the apparatus. For 52 weeks of exposure, 40 hours per week, the minimum allowable occupational distance is about 146 cm (4.8 feet). Note that this is based on continuous use, *i.e.*, worst case scenario. This allowable distance can be decreased by optimizing the source strength, and adequate shielding of the source.

Limitations And Conclusions

Limitations

The technique appears to have certain limitations, including being incapable of detecting very thin or porous occlusions, locating pitting of the pipe wall, and detecting small to moderate reduction of the pipe wall thickness. Although theoretically feasible, experiments could not reveal the thickness of porous corrosion blisters 0.6 cm thick. The apparatus, in its present form, is heavy for performing field experiments.

Being a feasibility study, this work did not include searching for possible solutions to these limitations. Future work is needed to investigate such issues.

The substantial source strength required for the scanning of sprinkler piping call's for training and licensing requirements for the field or laboratory application. Licensing and training add to the cost. However, there are cases which justify the added cost.

Conclusions

Determination of sprinkler piping occlusions and pipe wall degradation were investigated by using a non-invasive gamma-ray scanning technique. Theoretical and experimental investigations illustrated that the technique is capable of revealing the thickness, location, density and shape

of substantial solid occlusions without requiring any prior knowledge about the pipe interior. Major degradation of the pipe wall can also be determined with this technique, provided the scanning speed and collimator thickness are selected properly.

The scan plot of the controlled artificial samples matched closely with theory and produced sharp distinct interfaces. The natural samples provided less precise but useful results in that the occlusion/fluid interface could be detected sufficiently well to determine the hydraulic diameter of pipes occluded by solid, *e.g.*, non-porous, material.

While theoretically feasible, determination of thin and porous occlusions could not be achieved experimentally.

The resolution of the scan plots can be improved by increasing the detection efficiency, the source strength, and the area of the collimator, and by decreasing the scanning speed and the collimator width. Slit shaped collimators resulted far better resolutions than circular collimators. The technique can be successfully applied to pipes containing water and to empty pipes. However, low density occlusions can be detected more clearly when the pipe is empty.

REFERENCES

1. Schultz, G. R. "Water Distribution Systems," *Fire Protection Handbook*, Seventeenth Edition, National Fire Protection Association (NFPA), Quincy, MA, 1991, p. 5–51.

2. "Automatic Sprinkler Tables, 1970 Edition," *Fire Journal*, July 1970, p. 35.

3. *NFPA-13A, Recommended Practice for the Inspection, Testing, and Maintenance of Sprinkler Systems*, Quincy, MA, 1991 Edition.

4. Alipour-fard, M., *Identification of Wall Degradation and Occlusion in Fire Protection Piping Systems Using Gamma-ray Scanning*, M.S. Thesis, Worcester Polytechnic Institute, Worcester, MA, 1988.

5. Costello, J.J. "Postprecipitation in Distribution Lines Following Water Treatment," *Proceedings of American Water Works Association (AWWA) 1982 Annual Conference*, Miami Beach, FL, May 16–20, 1982.

6. Holler, A.C. "Corrosion of Water Pipes," *Journal of AWWA*, August 1974, p. 456.

7. Rothwell, G.P., "Corrosion Mechanisms Applicable to Metallic Pipes," *Corrosion Prevention and Control*, Vol. 26, No. 3, June 1979.

8. Lee, S.H., *et. al.*, "Biologically Mediated Corrosion and Its Effects on Water Quality in Distribution Systems," *Journal of AWWA*, November 1980, p. 636–645.

9. Vollmer, E., *Encyclopedia of Hydraulics, Soil, and Foundation Engineering*, Elsevier Publishing Company, 1967, p. 267.

10. Hodnett, R. M., "Care and Maintenance of Water-Based Extinguishing Systems," *Fire Protection Handbook*, Sixteenth Edition, National Fire Protection Association, Quincy, MA, 1986, p. 18–91 to 18–93.

11. Lapp, R. E. and Andrews, H. L., *Nuclear Radiation Physics*, Fourth Edition, Prentice Hall Inc., 1972.

12. Cember, H., *Introduction to Health Physics*, Second Edition, Pergamon Press, 1983.

13. Mayer, J. A. Jr., *GAMSCAN Computer Program*, Mechanical Engineering Department, Worcester Polytechnic Institute, Worcester, MA, 1987.